JOURNAL OF COMPUTATIONAL PHYSICS 31, 76–95 (1979)

# The "Cloud in Cell" Technique Applied to the Roll Up of Vortex Sheets

GREGORY R. BAKER

*Applied Mathematics, California Institute of Technology, Pasadena, California 91125*

Received April 18, 1977; revised April 13, 1978

The problem of the roll up of a two dimensional vortex sheet generated by a wing in an ideal fluid is phrased in terms of the streamfunction and the vortex sheet strength. A numerical method is used to calculate the time evolution of the vortex sheet by adapting the "Cloud In Cell" technique introduced in solving many particle simulations in plasma physics (see J. P. Christiansen, *J. Computational Physics 13* (1973)). Two cases are considered for the initial distribution of circulation, one corresponding to an elliptically loaded wing and the other simulating the wing with a flap deployed. Results indicate that small scale behaviour plays an important part in the roll up. Typically, small scale perturbations result in small structures which evolve into ever increasing larger structures by vortex amalgamation. Conclusions are given from a number of tests exploring the validity of the method. Briefly, small scale perturbations are introduced artificially by the grid; but once the process of vortex amalgamation is well underway, the emerging large scale behaviour is relatively insensitive to the precise details of the initial perturbations. Since clearly defined structures result from the application of this method, it promises to aid considerably in understanding the behaviour of vortex wakes.

## I. INTRODUCTION

When a wing of finite span moves at a small angle of attack through the air, it sheds vorticity at its trailing edge which results from the flow of air around the wing tip, driven by the pressure difference between the top and bottom surface of the wing. If the speed of the wing is constant and the effect of the viscosity of the air is negligible, vortex lines starting from the trailing edge form a steady surface relative to the wing, which is sharply defined and represents a vortex sheet.

The intractible problem of determining the location of this three dimensional steady vortex sheet is simplified by considering the sheet two dimensional and unsteady through the relation $z = Ut$ (see Fig. 1). This assumption ignores the curvature of the vortex lines and their termination at the trailing edge, and the relation $z = Ut$ assumes there is no variation of the velocity parallel to the $z$ axis. This proves reasonable when sufficiently far downstream of the wing, and Moore and Saffman [1] have provided formal justification. The variation of the vortex sheet strength shed at the trailing edge of the wing depends on the characteristics of the wing and becomes the initial condition for the unsteady problem. This paper examines two cases of initial



0021-9991/79/040076–20$02.00/0

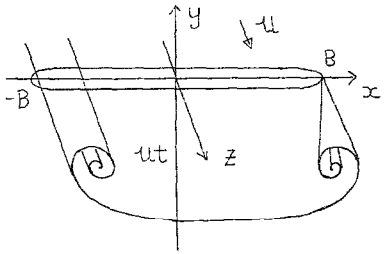


FIG. 1. The geometries for the three dimensional steady flow and two dimensional unsteady motion.

vortex sheet strength; one relates to an elliptically loaded wing and the other simulates a wing with a flap deployed.

Before introducing the method described in this paper, it is instructive to recall previous attempts at solving the model problem. For the elliptically loaded wing, the vortex sheet strength is initially infinite at the wing tip. The subsequent motion is the formation of a spiral at the wing tip with infinite arclength so that the singular nature of the initial flow is removed. Kaden [2] has presented the leading term of an asymptotic expansion describing the spiral and, more recently, further terms have been calculated [3, 4]. However, the asymptotic expansion contains unknown parameters which are determined by the flow outside the spiral. In particular, the location of the spiral center is unknown. Thus a numerical procedure is required to fully determine the motion.

In studying the Kelvin-Helmholtz Instability, Rosenhead [5] replaced the vortex sheet by a finite collection of line or point vortices and considered their subsequent motion as marking out the vortex sheet. Westwater [6] was the first to apply this approach to the vortex sheet rollup behind a wing. With the advent of high speed computers, a number of researchers [7–10] have continued this approach but an unsatisfactory feature of the results consistently emerges. The motion of the point vortices becomes chaotic in the region of the spiral. Different ad hoc modifications have been incorporated in an attempt to regularise the solution. Instead of point vortices, some authors [11, 12] introduced vortices with small but finite area. The velocity field in these cases is finite everywhere, but the distortion of the vortices by their mutual interaction is ignored and gives an error difficult to assess. A finite number of point vortices cannot adequately resolve the details of a spiral especially near its center. Moore [13] has addressed this aspect of the numerical calculation by incorporating an amalgamation process at the wing tip vortex. His spiral appears smooth for greater times than other calculations and more closely resembles the required asymptotic nature.

Unfortunately there has not yet been an adequate accounting of the errors introduced by these modifications. Fink and Soh [14] have pointed out that calculating the velocity at points on the sheet by considering them point vortices is not a good approximation unless the points are evenly spaced in arclength. Consequently, they

proposed a method which introduces evenly spaced points at each time level. For the roll up behind an alliptically loaded wing they obtain results very similar to Moore's [13], but this is a consequence of keeping the point closest to the spiral center fixed during the redefinition of points and assigning to it the vorticity necessary to conserve circulation. Thus, vorticity accumulates at this point in an ad hoc manner and this point becomes an approximation to the innermost turns of the spiral.

Baker [15] has extended their work by taking some account of the curvature of the sheet when calculating its velocity, resulting in a higher order of accuracy. He applied the refined method to the sheet shed by a ring wing because there is no singularity associated with a wing tip, and so this case provides a definite test of the method. The truncation error in calculating the velocity of the vortex sheet is of order of the cube of the spacing between points. There is no corresponding estimate for the truncation error when using point or discrete vortices. If a smooth, stable solution exists, increasing the number of points would lead to smaller corrections in the computed results. This is not the behavior observed irrespective of whether the basic or refined method is used. The vortex sheet's motion is calculated with different numbers of points and the results are compared at some chosen time during the initial stages of roll up. As the number of points increases, the spiral nature of the roll up becomes more prominent but the outer turns distort and intersect one another. No consistent solution emerges; the problem appears ill-posed.

Brown and van Dyke [35] also find that Fink and Soh's method proves inadequate in calculating the vortex sheet motion associated with a wing with flaps deployed, and Sarpkaya [36] reports no substantial improvement when using their method instead of the method of point vortices for the roll up of vortex sheets shed from an inclined plate in a uniform flow. If we are to find reliable numerical procedures, we need to understand the cause of breakdown commonly obtained. There are several possibilities as follows. The stability of the vortex is generally uncertain. The plane, constant sheet has a known instability, the Kelvin Helmholtz Instability [16], where the modes with the smallest wavelength grow the fastest. However, the effects of curvature and stretching of the sheet may be stabilising [17]. If the sheet is unstable, the numerical method will reflect this in the growth of round-off errors. In this case, the relevant problem is understanding the nonlinear development of the instability, and this requires a sufficient number of points to resolve the important modes. Alternatively, the numerical methods may be unstable independently of the stability of the sheet. The accurate calculation of the vortex sheet motion in the spiral region may require many points because of the close spacing between the turns and their large curvature.

Many of these questions can be explored by increasing the number of points substantially. Adopting a different procedure in calculating the vortex sheet velocity will also increase the breadth of inquiry and give useful information about the basic nature of its motion. This is also desirable for matters of economy. The computer time required to update the positions of $N$ point vortices is $O(N^3)$ since the system is stiff with shortest time scale $O(N^{-1})$, and this approach soon becomes expensive for large $N$. Adapting the "Cloud in Cell" technique ensures the calculation of the motion of many vorticity markers at reasonable cost. The purpose of this paper is to describe

the method and discuss the results obtained when applied to the roll up behind an elliptically loaded wing and behind a wing with a flap deployed. The conclusions from several tests to examine the accuracy and reliability of the method are also given.

This technique has already been applied to a number of two dimensional ideal fluid flows [18, 19]. These applications have yielded interesting results, in particular the behaviour of the interaction of finite sized vortex structures. Baker [15] used this technique in studying the motion of vortex sheets. Subsequently Meng and Thomson [34] have used a similar approach but there is no attempt to explore the errors in their scheme other than by comparison with results obtained with discrete vortices. The present work is a continuation of the study of the roll up of vortex sheets started by Baker [15] and it explores the validity of the "Cloud in Cell" technique for vortex sheet motion.

## II. The Method

Christiansen [18] was the first to report the use of the "Cloud in Cell" technique in studying the motion of a two dimensional, incompressible, inviscid and homogeneous fluid. A similar approach is used in this paper; the details are as follows.

If $\psi$ is the streamfunction, $\omega$ the vorticity, and $u$, $v$ the velocity components, the equations of motion are

$$\nabla^2\psi = -\omega \tag{1}$$

$$u = \frac{\partial\psi}{\partial y} \tag{2a}$$

$$v = -\frac{\partial\psi}{\partial x} \tag{2b}$$

$$\frac{\partial\omega}{\partial t} + u\frac{\partial\omega}{\partial x} + v\frac{\partial\omega}{\partial y} = 0. \tag{3}$$

The vorticity is discretised by introducing $N$ markers,

$$\omega = \sum_{n=1}^{N} \Gamma_n \delta(x - x_n)\,\delta(y - y_n) \tag{4}$$

such that

$$\sum_{n=1}^{N} \Gamma_n = \int \omega\, dA \tag{5}$$

This reduces Eq. (3) to a set of ordinary differential equations,

$$\frac{dx_n}{dt} = u(x_n, y_n) \tag{6a}$$

$$\frac{dy_n}{dt} = v(x_n, y_n) \tag{6b}$$

To obtain the streamfunction, a finite difference approximation is made to Eq. (1) on a rectangular grid, $\{x_0 + (i-1)H_x,\ y_0 + (j-1)H_y\}$, $1 \leqslant i \leqslant N_x$, $1 \leqslant j \leqslant N_y$, where $H_x$, $H_y$ are the grid spacings assumed uniform in the $x$, $y$ directions respectively.

$$(\psi_{i+1,j} - 2\psi_{i,j} + \psi_{i-1,j})/H_x^2 + (\psi_{i,j+1} - 2\psi_{i,j} + \psi_{i,j-1})/H_y^2 = -\omega_{i,j} \quad \text{for} \quad 2 \leqslant i \leqslant N_x - 1, \quad 2 \leqslant j \leqslant N_y - 1. \tag{7}$$

The vorticity is represented at the points $(x_n, y_n)$ and so a redistribution scheme, known as "Cloud in Cell" or area-weighting, is introduced to assign values at the grid points and then Eq. (7) can be solved. Fig. 2 provides the geometry and notation of the redistribution scheme,

$$\omega(k) = A_k \Gamma_n / H_x H_y \tag{8}$$

where the $A$'s are the areas shown. This scheme conserves total vorticity and the hydrodynamic impulse (related to linear momentum), but the angular impulse is changed by an amount bounded by $0.25\Gamma(H_x + H_y)$, where $\Gamma$ is the total circulation.

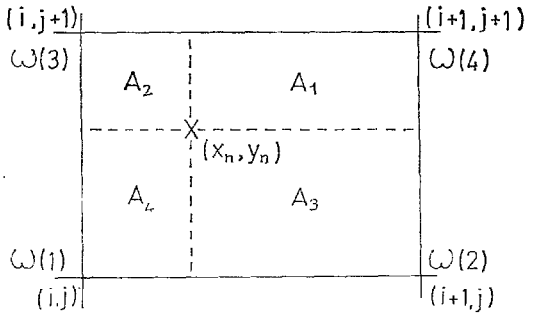


FIG. 2. The geometry and notion of the "Cloud in Cell" redistribution scheme.

Eq. (7) is easily solved using a Fast Poisson Solver (the FACR($l$) method [20] using a particular Fast Fourier Transform [21]). To determine the velocity of the markers, we calculate the velocity at the nearest four grid points with a central difference formula,

$$u_{i,j} = (\psi_{i,j+1} - \psi_{i,j-1})/2H_y \tag{9a}$$

$$v_{i,j} = -(\psi_{i+1,j} - \psi_{i-1,j})/2H_x \tag{9b}$$

and then interpolate bilinearly.

$$u_n = \left(\sum_{k=1}^{4} u(k)\, A_k\right) \Big/ H_x H_y \tag{10}$$

The notation of Fig. 2 has been followed in Eq. (10). The markers are moved forward in time by a finite difference approximation to Eq. (6).

$$x_n(t + \Delta t) = x_n(t) + u_n \Delta t \tag{11a}$$

$$y_n(t + \Delta t) = y_n(t) + v_n \Delta t \tag{11b}$$

where $\Delta t$, the time step, is chosen to satisfy

$$\Delta t < \operatorname*{Min}_n \left( \frac{H_x}{u_n}, \frac{H_y}{v_n} \right). \tag{12}$$

This condition is an analogue to the condition required for explicit finite difference approximations to Eq. (3), and hence appears plausible. However, there is no evidence that Eq. (12) is required and a larger $\Delta t$ may be permissible. In this way, the vorticity distribution at $t + \Delta t$ has been computed and the procedure repeats to give the motion of the vorticity.

Boundary conditions must be given at the grid edge for a unique solution. The author used a particular Fast Poisson Solver which requires the value of $\psi$ along the boundaries. These values of $\psi$ can be obtained in several ways. The author's choice is to calculate local centroids of vorticity

$$\bar{\Gamma}_m = \sum_{n=(m-1)p+1}^{mp} \Gamma_n \tag{13a}$$

$$\bar{\Gamma}_n \bar{x}_m = \sum_{n=(m-1)p+1}^{mp} x_n \Gamma_n \tag{13b}$$

$$\bar{\Gamma}_m \bar{y}_m = \sum_{n=(m-1)p+1}^{mp} y_n \Gamma_n \tag{13c}$$

where $m = 1, 2, \ldots, M = N/p$. The velocity at the boundary is determined by regarding these local centroids as point vortices. Maskew [22] indicates that the resulting error is small when the boundary is a distance $1.5H$ away from the nearest vortex marker $(x_n, y_n)$ where $H$ is the maximum distance between adjacent local centroids $(\bar{x}_m, \bar{y}_m)$. In fact, this is the criterion used to choose the location of the boundaries of the grid to minimize the region in which the solution of Eq. (1) is sought without loss of accuracy, given the number of local centroids. Keeping the boundaries away from the region of vorticity also ensures the conservation of vorticity, hydrodynamic impulse and the Kirchhoff-Routh path function.

Increasing the number of local centroids increases the accuracy but also the computing time and so a judicious choice is required depending upon the problem at hand. To decrease computer time, the velocity is calculated at a selected number of grid points at the boundary and the rest of the values are obtained by interpolation using cubic splines [23]. The appropriate component of velocity is integrated numerically using the trapezoidal rule around the boundary to provide the streamfunction. Since

it is singlevalued, it must return to its starting value after a complete circuit around the boundary and this provides a check on the accuracy. For 40 local centroids in a mesh $129 \times 129$, the typical relative error is $0(10^{-3})$. When the flow has a plane of symmetry, a boundary can be chosen along this plane. Since it is also a streamline, a prescribed constant value can be assigned to the streamfunction along this boundary.

Hockney [20] describes an alternative method to determine the streamline at the boundary, which uses an expansion in the inverse of the distance from the center of the grid. The calculation of $L$ coefficients of this expansion requires $O(LN_xN_y)$ computer operations which is much larger than the $O[M(N_x + N_y)]$ operations in using local centroids, when $M$ is reasonably smaller than $N_x$ or $N_y$. Both of these methods are much faster than enclosing the region of interest in a periodic box and using Fast Fourier Transforms [20]. Thus the method employed is the most economical without sacrifice of accuracy, known to the author.

It is natural to ask which aspect of the procedure limits the accuracy of the numerical solution. Since a vortex sheet is smeared over a region of the order of cell area, the grid spacing is expected to play an important role. In fact, Langdon [24] presents an analysis of grid effects in calculating the velocity and shows that this is the case. The author conducted several tests on particular vortex sheets where the velocity field is known analytically at a fixed time. Typically, the calculated sheet velocity resembles the exact velocity, superimposed with a small random component whose wavelength is of the order of the grid spacing. This behaviour is most likely a result of the bilinear interpolation used when computing the velocity at the vortex markers. However, it is the growth of the errors in the position of the sheet that is important and Langdon's [24] analysis does not fully address this aspect of the numerics.

A number of authors [24–27] have explored the errors arising in the "Cloud in Cell" and related methods when applied to the flow of particles in a plasma. They are concerned with the accuracy of representation of the Coulombic force law between charged particles and have shown how this force is modified by the different redistribution techniques. Their particles have a physical reality. Vortex markers on the other hand are a result of a numerical discretisation. In other words, whereas the motion of charged particles is the underlying structure to the continuum equations in plasma physics, point vortices are only a numerical representation of continuous vorticity distributions. The main question is how well does the "Cloud in Cell" method approximate the motion of continuous vorticity distributions. At present, analysis does not answer this question, and the best approach is to test the method on flows where some information is available.

## III. Testing the Method

The initial unstable motion of the infinitesimally perturbed plane constant vortex sheet (the Kelvin Helmholtz instability [16]) is known analytically; the growth rate is proportional to the wave number. A sinusoidal perturbation with an amplitude 0.01 and unit wavelength is taken as the initial condition for test runs. At each time step,

a cubic spline [22] is fitted through the vorticity markers $(x_n, y_n)$ as an approximation to the sheet. Provided the sheet is singlevalued, the amplitudes of the Fourier modes are calculated by using Fast Fourier Transforms [21]. The calculated behaviour of the amplitudes is then compared with theory.

Two of the grid boundaries are chosen one wavelength of the imposed perturbation apart, and periodic conditions are applied in this direction on these boundaries. The number of vorticity markers and grid intervals are separately varied to observe their influence on the sheet motion. The timestep is reduced well below the necessary value for accuracy to study the initial motion in detail. The sheet develops small scale instabilities of the order of the grid spacing, and the way this occurs proves interesting.

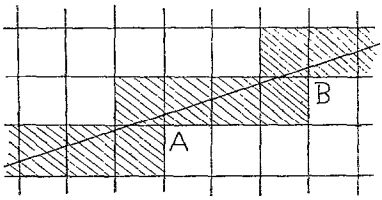


FIG. 3. Cells affected in redistribution process.

Fig. 3 shows a vortex sheet intersecting grid lines. The cells in which redistribution takes place are shaded. The smooth vortex sheet is replaced by a jagged array of cells, and it is at the places marked $A$ and $B$, for instance, that the biggest perturbation to the sheet occurs due to the anistropic redistribution process. The distance $AB$ is the dominant small scale introduced, while other small scales are essentially suppressed. By that it is meant that structures are formed along the sheet at places such as $A$ and $B$, which initially resemble small spirals, and the sheet is relatively smooth between them. This effect of the grid has been seen before, but in a less obvious way and merely reported as an anomalous instability [18].

The grid is refined from $17 \times 17$ through to $129 \times 129$, and the dominant small scale wavenumber increases as more grid lines intersect the sheet. The small scales also occur at earlier times and both these effects can be seen in Fig. 4, which shows the position of the sheet at $t = 0.06/U$ where $2U$ is the jump in velocity across the unperturbed sheet. The large scales related to the sinusoidal perturbation have growth rates in good agreement with non-linear theory to second order terms in the perturbation amplitude, higher order terms being negligible. Provided the number of vorticity markers is greater than two per cell, it has little influence on the large scale motion, but it does affect the detailed description of the smaller scales.

To check the time integration, the leap-frog scheme was substituted for Eq. (11) with little change in results. However, at the suggestion of a referee, further tests were conducted using a modified Euler integration, i.e.,

$$\bar{x}_n = x_n(t) + u_n(x_n)\,\Delta t \tag{14a}$$

$$x_n(t + \Delta t) = x_n(t) + 0.5(u_n(x_n) + u_n(\bar{x}_n))\,\Delta t \tag{14b}$$

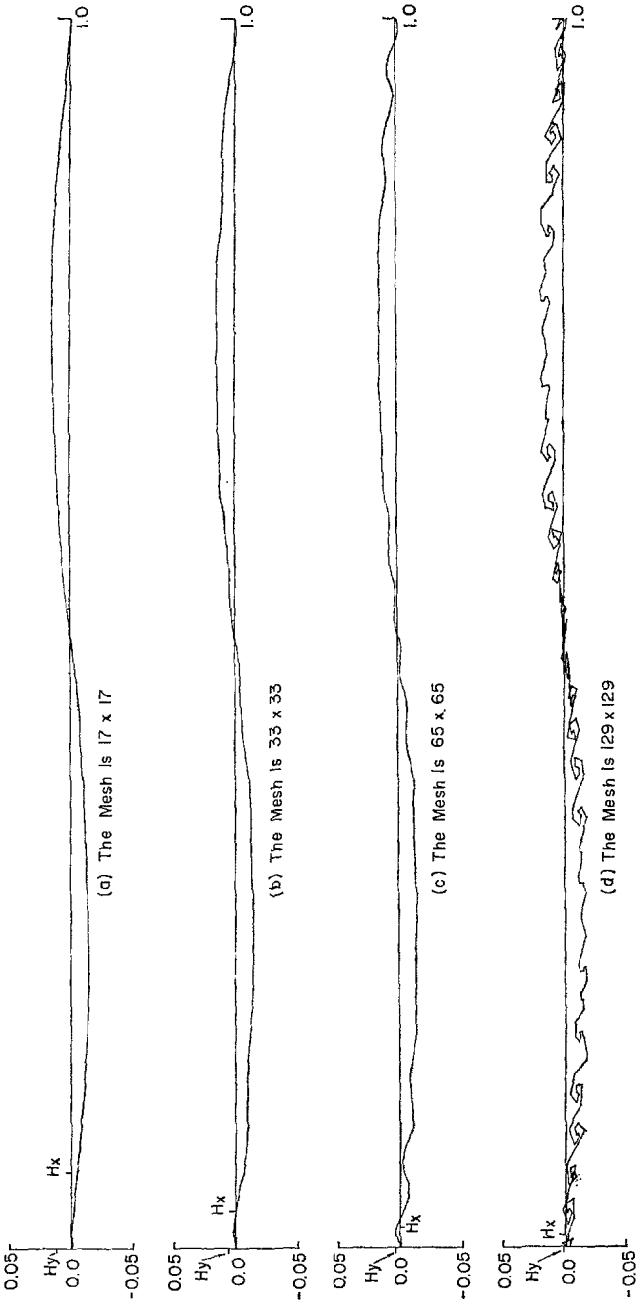


FIG. 4. Position of the vortex sheet at $t = 0.06/U$ for varying grid sizes. Number of vortex markers is 256, and $H_x$, $H_y$ refer to the size of an actual grid cell.

and similarly for $u_n(t + \Delta t)$. This method is stable and second order accurate. No change was observed in the generation of small scale structures and the only change in the large scale behaviour was a slight ($\sim$10 %) decrease in the size of the wing tip vortex structure. The significant difference was an improvement in the vorticity distribution at the center of the wing tip vortex structure, and this difference will be emphasized in the following sections where appropriate, while Eq. (11) is used for the time integration for economical reasons since Eq. (14) requires twice as many velocity determinations. However, for calculations requiring internal details of the vortex structures, it is recommended that Eq. (14) be used.

The conclusion of these tests is that the large scale sheet motion is accurately calculated, but that small scale perturbations are introduced artificially by the grid. The perturbations initially take on the form of small spirals, but the sheet soon loses its definition and small scale structures appear. These structures then amalgamate in a manner reminiscentjof the mixing layer [29, 30]. Thus the technique may lead to an adequate description of the final vortex structure and this aspect is considered in the applications described below.

## IV. First Application

The vortex sheet lies initially along $-B < x < B$, $y = 0$ and has strength related to the circulation shed at the trailing edge. For an elliptically loaded wing, this circulation is

$$\Gamma(x) = -2V_0B(1 - (x/B)^2)^{1/2} \tag{15}$$

where $V_0$ is the initial downwash velocity. Non-dimensional variables are introduced by scaling distances with $B$, time with $B/V_0$ and the circulation with $V_0B$. Eq. (15) reads

$$\Gamma(x) = -2(1 - x^2)^{1/2} \tag{16}$$

The results are shown as a series of vorticity distributions at different time levels in Fig. 5. The number of points used is 2000 each representing the same amount of circulation, but only half are plotted for practical purposes. The grid size is 129 $\times$ 129, and with 40 local centroids, it takes 3.2 secs. on an IBM 370/158 computer to update the velocity markers; 1.7 secs. of this is spent in solving Poisson's equation. The most striking features are the emergence of small scale structure and the smoothing of the spiral core. The large scale structure stays well defined, even though small scale structures developed outside the spiral region are convected into it and absorbed. This behavior is pleasingly similar to some experimental observations [28]. It is interesting to note that the small scale structures emerge first in regions where the motion of point vortices becomes chaotic in previous work, that is, inside the spiral and on the lower part of the outer arm of the spiral [13].

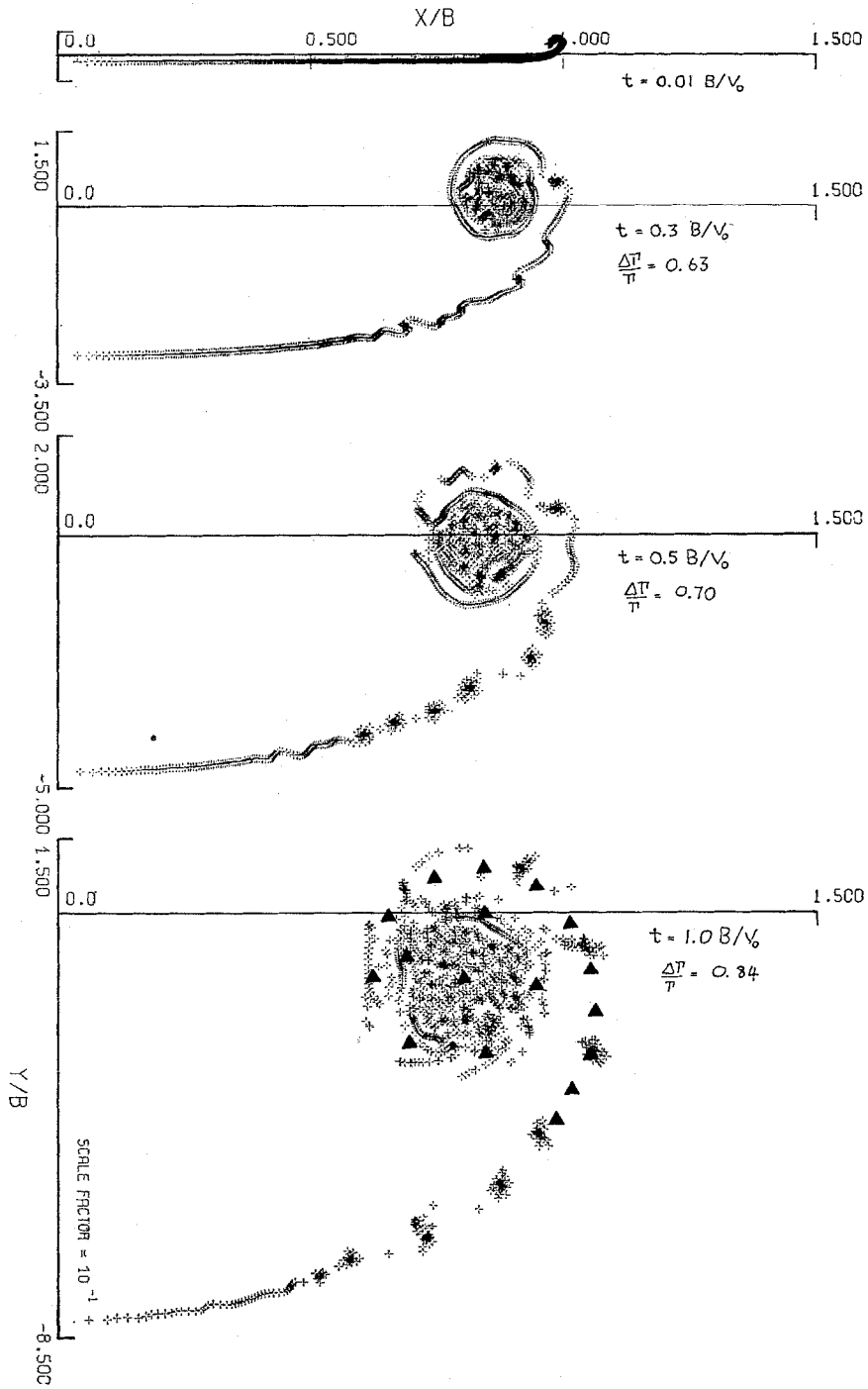


FIG. 5. Vorticity distributions for the roll up behind an elliptically loaded wing at different times, $V_0 t/B = 0.10, 0.3, 0.5, 1.0$.

As a check on the accuracy of the method, two invariants of the motion are monitored during the calculation. One is the spanwise component of the hydrodynamic impulse and its computed value has a relative error of $10^{-4}$. The Kirchhoff–Routh path function is the other, but the computed value varies slowly with time. Since it proves too expensive to calculate this function for the complete collection of vorticity markers, only local centroids are used and a 10 % relative error was found. Tests indicate that the error decreases when more points are included. Although the computed function is approximate, its slow variation suggests reasonable invariance.

Superimposed on the vorticity distribution at time $t = 1.0\ B/V_0$ in Fig. 5 are the positions of the point vortices obtained by Moore [13] in the vicinity of vortex structure. The agreement is good despite the use of Eq. 11 for the time integration whereas Moore used a more accurate Runge–Kutta scheme. If Eq. 14 is used for the time integration, the vorticity is more concentrated at the center of the wing tip vortex with a smaller area of uniform vorticity. The fall off in the vorticity distribution in the outer regions of the structure follows more closely the inviscid predictions.

The fraction of vorticity rolled up is also calculated using a definition given by Moore [13], that is, the fraction of markers with $n \geqslant N$ where $N$ is determined from $x_N = \max x_n$, and increasing $n$ counts markers along the sheet towards the core center. This fraction is shown in Fig. 6 as a function of time. Initially the behaviour follows the similarity solution [2] and agrees well with Moore's results. Thus the gross features obtained by point vortices are reproduced. The slight oscillation observed is due to the convection of small structures around and into the roll up region.

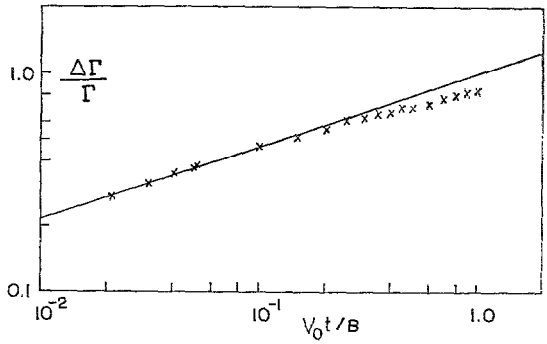


FIG. 6. Fraction of circulation in roll up region as a function of time. Slope of straight line is from Kaden's similarity solution.

Another aspect of the results is presented in the velocity profiles shown in Fig. 7. They are spanwise scans through the core center of the vertical velocity component and are a measure of the tangential velocity around the core. The times chosen correspond to two of the four time levels in Fig. 5. Turns of the spiral and small scale structure at the core edge are evident by double peaks. The inner region resembles solid body rotation and this is consistent with radial profiles of the vorticity measured from the core center. The size of the inner region is decreased when using Eq. 14

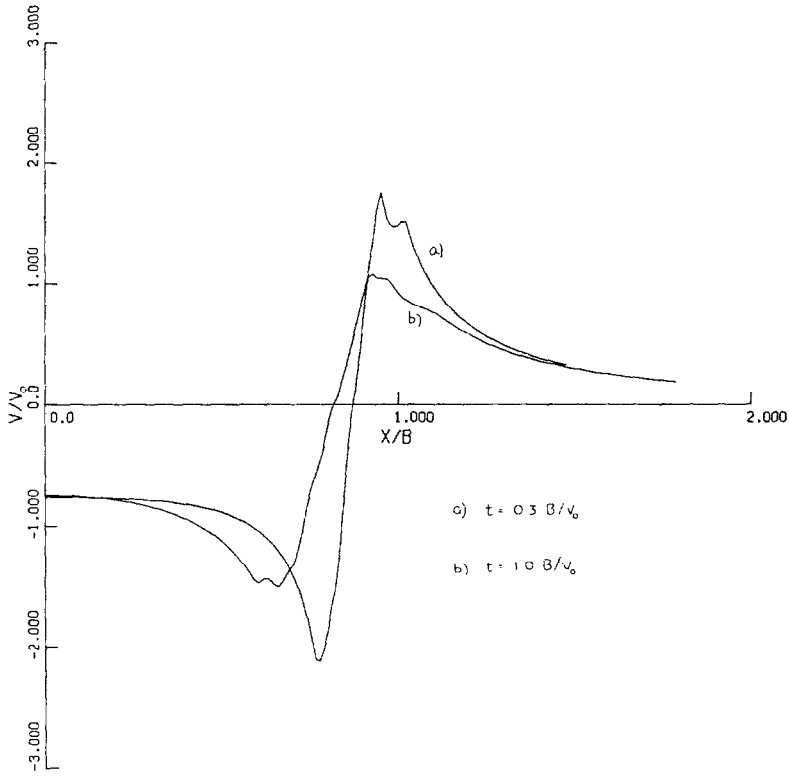


FIG. 7. Vertical velocity profiles in the spanwise direction through the core center.

instead of Eq. 11 leading to larger velocity peaks and narrower distances between maximum and minimum velocities.

The maximum difference in the vertical velocity at a fixed time is a measure of the evolution of the vortex structure. Its time dependence is very close to a decay as $t^{-1/4}$, and this is predicted for a vortex structure with a viscous core matched to an outer flow specified by the similarity solution [1]. Moreover, the viscous core has solid body rotation at its center. This interesting parallel in behavior of the results deserves attention.

We emphasize that the "Cloud in Cell" technique has produced a well defined rolled up structure.

## V. SECOND APPLICATION

The second application of the method shows an interesting difference in the roll up of different parts of the vortex sheet. An initial circulation distribution is chosen by matching three sections so that the circulation and its derivative are continuous.

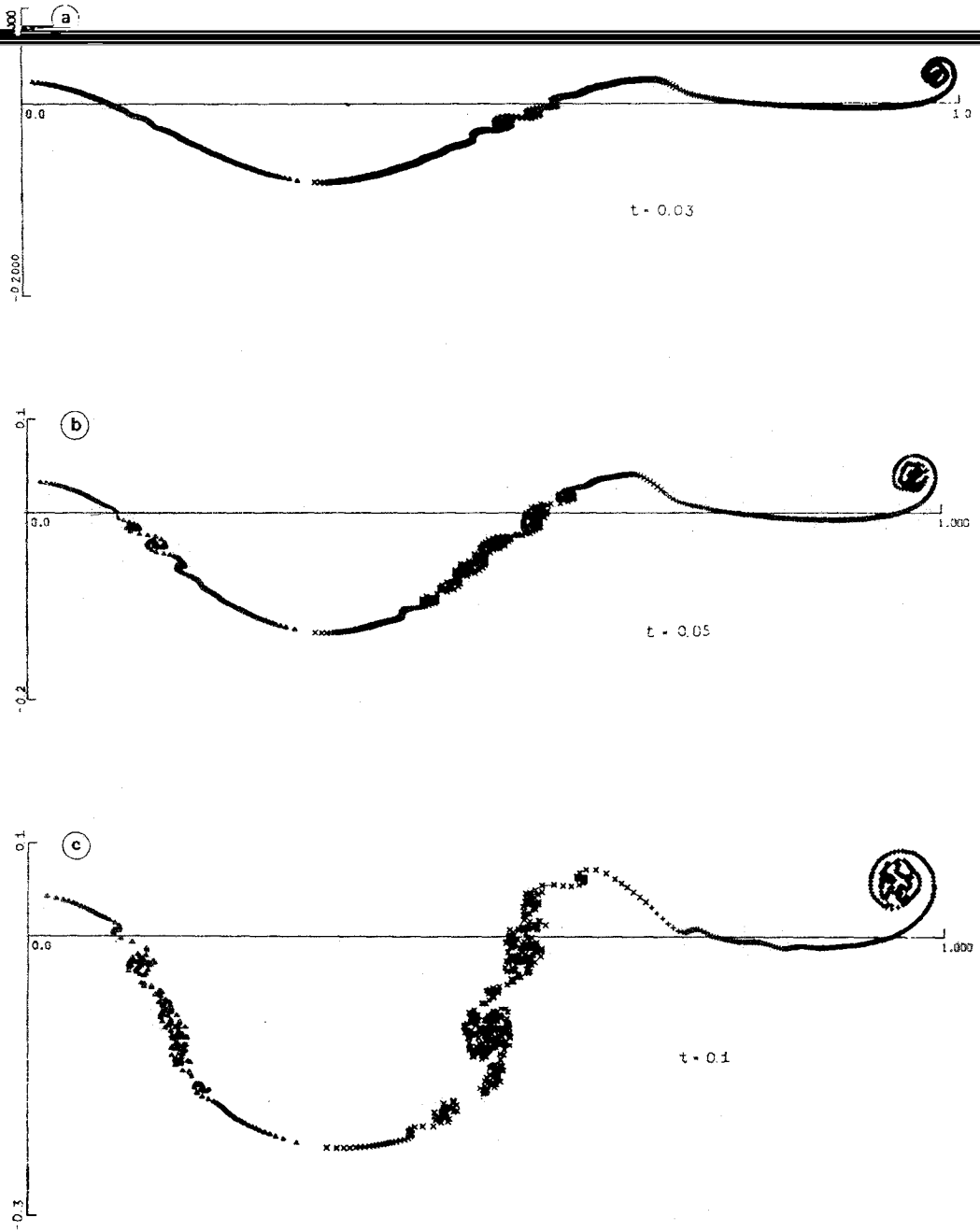


FIG. 8. Vorticity distribution for the roll up behind a wing with with a flap deployed at different time levels. The grid is 129 × 129. (a) $t = 0.03$, (b) $t = 0.05$, (c) $t = 0.1$, (d) $t = 0.15$, (e) $t = 0.2$, (f) $t = 0.3$.

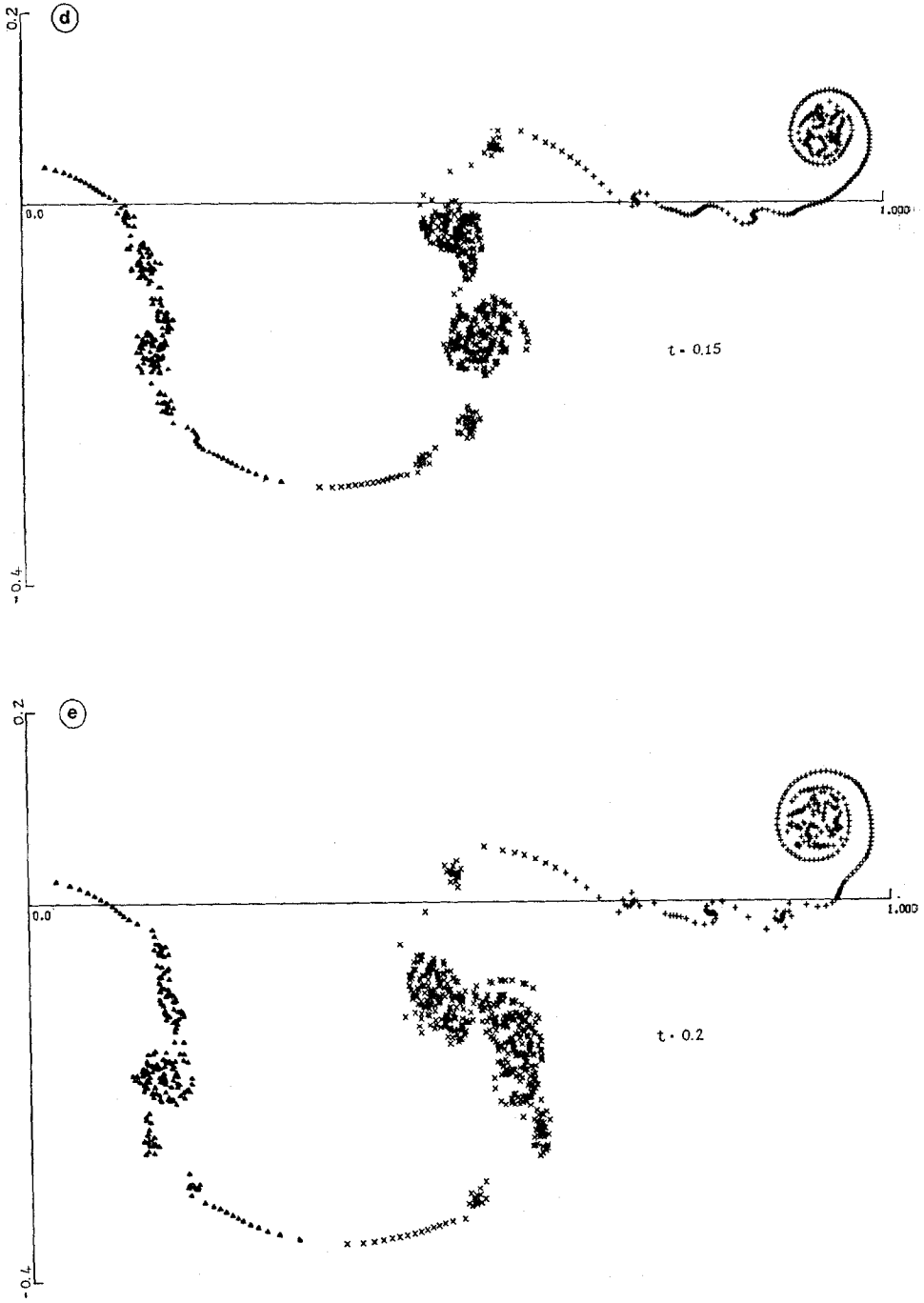


Fig. 8 (*continued*)

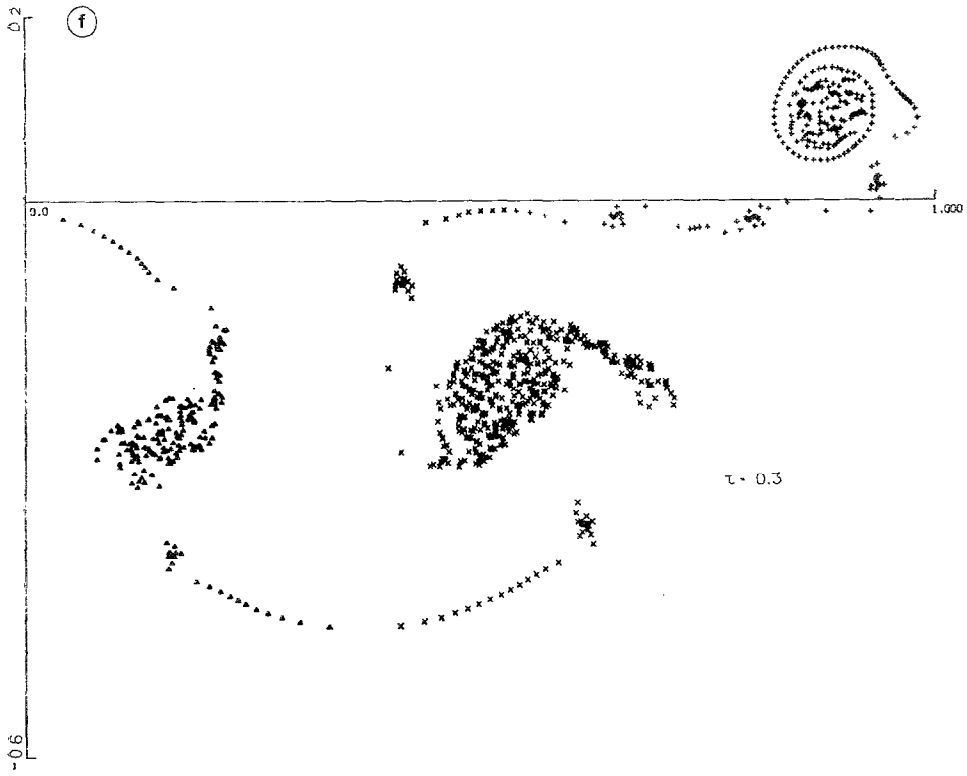


Fig. 8 (*continued*)

For $0 \leqslant x \leqslant A$,

$$\Gamma(x) = \Gamma_0 + \frac{3}{A^2}(\Gamma_1 - \Gamma_0)\,x^2 - \frac{2}{A^3}(\Gamma_1 - \Gamma_0)\,x^3 \tag{17a}$$

where $\Gamma_1$ is the maximum circulation. For $A \leqslant x \leqslant B$,

$$\Gamma(x) = ax^3 + bx^2 + cx + d \tag{17b}$$

where $a = -2[\Gamma_1 - (1 - B^2)^{1/2}]/(A - B)^3 - B/[(1 - B^2)^{1/2}(A - B)^2]$, $b = B/[2(1 - B^2)^{1/2}(A - B)] - 3A(A + B)/2$, $c = -3aA^2 - 2bA$, $d = \Gamma_1 - aA^3 - bA^2 - cA$. For $B \leqslant x \leqslant 1$, elliptical loading is assumed,

$$\Gamma(x) = (1 - x^2)^{1/2} \tag{17c}$$

This profile simulates the effect of a deployed flap and the influence of the fuselage near $x = 0$. Roughly speaking, the fuselage influences the region, $0 < x < A$, the outboard edge of the flap the region, $A < x < B$, and the wing tip the region, $B < x < 1$. The values chosen for the constants are $A = 0.3$, $B = 0.7$, $\Gamma_0 = 1.4$,

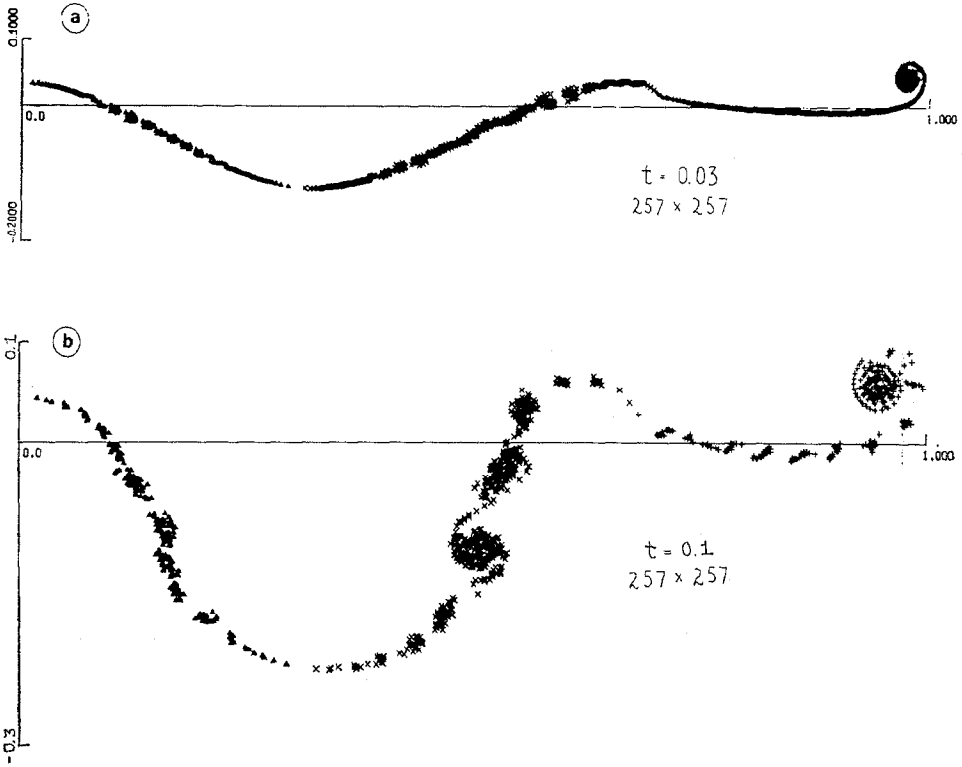


FIG. 9. The same as Figs. 8a and c with refined grid, 257 × 257.

$\Gamma_1 = 2.0$, where the units are arbitrary since the interest is to demonstrate the feasibility of the method rather than to obtain precise results. For this configuration three vortex structures are observed to develop, and Donaldson [31] has proposed a criterion which determines which part of the initial vortex sheet is later rolled up into these structures. His criterion corresponds to the regions defined by Eq. (17).

Fig. 8 gives the vorticity distribution as time progresses and indeed three structures emerge. The grid is 129 × 129 and the total number of points, again with equal circulation, is 1950; 450 for the fuselage region, 964 for the flap region and 536 for the tip region. Only half the points are plotted and they are marked in different symbols for each region. The results show that the points $A$ and $B$ are the appropriate demarcation of the initial circulation profile as proposed in [31].

Unlike the tip vortex, the fuselage and flap vortices emerge by an amalgamation process more reminiscent of the process in a mixing layer than the formation of a spiral. However the final structures have a form similar to the tip vortex. Since the initial development of the small scales is grid dependent, an important test of the results is to repeat the calculation with a finer grid. Fig. 9 shows the result for a grid, 257 × 257, at the same times as Fig. 8a and 8c. Although the initial small scale

structures are different and occur at an earlier time, the emerging large scale structure has remarkable similarity. Even during the intermediatary stages of amalgamation, the vorticity distribution appears reproduced. This illustrates the result found in independent testing, namely that large scale motion is accurately computed.

Finally, a comment is in order about the behaviour of the angular momentum for both flows considered in this paper. The angular momentum for the region $x > 0$ is not an invariant of the motion. Milinazzo and Saffman [32] have shown that the angular momentum is reliably calculated by the "Cloud in Cell" technique. For an elliptically loaded wing, the angular momentum about the centroid increases by 35 % at $t = 1.0$ when the roll up is almost completed (fraction of rolled up vorticity is 85 %). This indicates a limitation to the Betz approximation [33]. For the case of a wing with a flap deployed, the angular momentum about the centroids of each region is shown in Fig. 10. This is in sharp disagreement with the extension of the Betz approximation [31] and indicates a better understanding for the case of the roll up with more than just a tip vortex may be required. Of course the dissipative process involved in the method will influence the angular momentum and that should be born in mind when comparing with inviscid estimates.

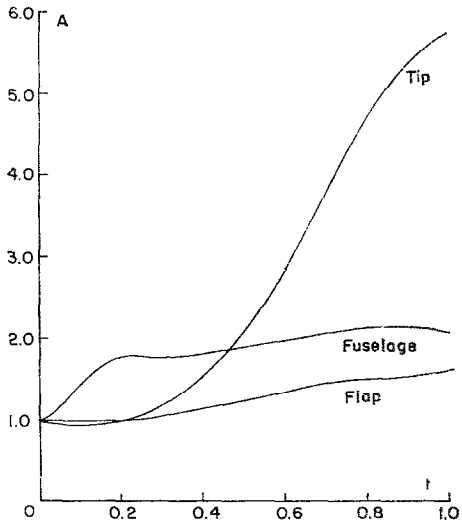


FIG. 10. Angular momentum, $A$, normalized by its initial value for the three vortex structures as a function of time.

## VI. CONCLUSION

The "Cloud in Cell" technique produces interesting results for the motion of vortex sheets. In particular small scale instabilities introduced by the grid destroy the definition of the sheet, but a process of amalgamation which is relatively insensitive to the

grid results in the emergence of large scale vortex structures, which are clearly defined since many vorticity markers can be used without high computing costs. The computation can be continued if the study of the interaction of these structures is required. The properties of these structures agree well with previous calculations of vortex sheet motion using point vortices.

The main disadvantage in using this technique is the loss of detail of the spiral nature of the vortex sheet roll up. Algorithms can be introduced which prevent the vortex sheet from kinking and which may lead to more clearly described spirals. However it is strongly recommended that more detailed studies of the numerical errors are required before ad hoc modifications are introduced to reproduce "expected" vortex sheet behavior. For these reasons, this technique holds good prospects for improving our understanding of vortex sheet roll up.

## ACKNOWLEDGMENTS

I wish to thank Professor Philip G. Saffman for many helpful discussions and Professor Bengt Fornberg for assistance with computer programming.

This work was supported by the Energy Research Development Administration (AT 04-3-767) and the U.S. Army Research Office, Durham (DAHC 04-68-C-0006).

## REFERENCES

1. D. W. MOORE AND P. G. SAFFMAN, *Proc. Roy. Soc. London Ser. A* **333** (1973).
2. H. KADEN, *Ing. Arch.* **2** (1931), 140 (English trans., R.A.E. Library Trans. No. 403).
3. D. W. MOORE, *Proc. Roy. Soc. London Ser. A* **345** (1975), 417.
4. J. P. GUIRAUD AND R. KH. ZEYTOUNIAN, *J. Fluid Mech.* **79** (1977), 93.
5. L. ROSENHEAD, *Proc. Roy. Soc. London, Ser. A* **134** (1931), 170.
6. F. L. WESTWATER, Aero. Res. Counc. R & M. No. 1962, 1935.
7. G. D. BIRKHOFF AND J. FISHER, *Rend. Circ. Mat. Palermo* **8**(2) (1959), 77.
8. H. TAKAMI, Rep. SUDAER (202), Stanford University, Stanford, Calif. 1964.
9. D. W. MOORE, California Institute of Technology, Pasadena, California Institute of Technology, Pasadena, Calif., 1971.
10. R. R. CLEMENTS AND D. J. MAULL, *J. Roy. Aeronaut. Soc.* **77** (1973), 46.
11. K. KUWAHARA AND H. TAKAMI, *J. Phys. Soc. Japan* **34** (1973), 247.
12. A. J. CHORIN AND P. S. BERNARD, *J. Computational Phys.* **13** (1973), 423.
13. D. W. MOORE, *J. Fluid Mech.* **63** (1974), 225.
14. P. T. FINK AND W. K. SOH, Tenth Symposium on Naval Hydrodynamics, Cambridge, Mass., 1974.
15. G. R. BAKER, Ph.D. thesis, Applied Math. Dept., California Institute of Technology, Pasadena, Calif., 1977.
16. G. K. BATCHELOR, "An Introduction to Fluid Dynamics," p. 511, Cambridge University Press, London/New York, 1970.
17. D. W. MOORE, *Mathematika* **23** (1976), 35.
18. J. P. CHRISTIANSEN, *J. Computational Phys.* **13** (1973), 363.
19. J. P. CHRISTIANSEN AND N. J. ZABUSKY, *J. Fluid Mech.* **61** (1973), 219.
20. R. W. HOCKNEY, *in* "Methods of Computational Physics," (B. Alder, S. Fernbach, and M. Rotenberg, Eds.), Vol. 9, Academic Press, New York, 1970.

21. B. FORNBERG, *J. Computational Phys.* **25** (1977), 1.

23. T. W. HAMMING, "Numerical Methods for Scientists and Engineers," 2nd ed., p. 349, McGraw–Hill, 1973.
24. A. B. LANGDON, *J. Computational Phys.* **6** (1970), 247.
25. C. K. BIRDSALL AND D. FUSS, *J. Computational Phys.* **3** (1969), 494.
26. J. W. EASTWOOD, *J. Computational Phys.* **18** (1975), 1.
27. J. W. EASTWOOD AND R. W. HOCKNEY, *J. Computational Phys.* **16** (1974), 342.
28. D. PIERCE, *J. Fluid Mech.* **11** (1961), 460.
29. G. L. BROWN AND A. ROSHKO, *J. Fluid Mech.* **64** (1974), 775.
30. C. D. WINANT AND F. K. BROWNAND, *J. Fluid Mech.* **63** (1974), 237.
31. C. DUP. DONALDSON, R. S. SNEDEKER, AND R. D. SULLIVAN, *J. Aircr.* **11** (1974), 547.
32. F. MILINAZZO AND P. G. SAFFMAN, *J. Computational* **23** (1977), 380.
33. A. BETZ, TM 713, June 1933, NACA.
34. J. C. S. MENG AND J. A. L. THOMSON, *J. Fluid Mech.* **84** (1978), 433.
35. C. E. BROWN AND P. VAN DYKE, AFOSR-TR-76-0481, Hydronautics Inc., Laurel, Md., 1976.
36. T. SARPKAYA, *AIAA J.* **13** (1975), 1680.